Reopen Schools Safely: Simulating COVID-19 Transmission on Campus With a Contact Network Agent-based Model

Chuyao Liao
Sun Yat-sen University
Xiang Chen
University of Connecticut
Li Zhuo (zhuoli@mail.sysu.edu.cn)
Sun Yat-sen University
Yuan Liu
Sun Yat-sen University
Haiyan Tao
Sun Yat-sen University

Research Article

Keywords: COVID-19, contact network, vaccination, agent-based modeling, school

Posted Date: June 30th, 2021

DOI: https://doi.org/10.21203/rs.3.rs-627505/v1

Version of Record: A version of this preprint was published at International Journal of Digital Earth on February 10th, 2022. See the published version at https://doi.org/10.1080/17538947.2022.2032419.

Abstract

Background: As phases of COVID-19 vaccination are quickly rolling out, how to evaluate the vaccination effects and then make safe reopening plans has become a prime concern for local governments and school officials.

Methods: We develop a contact network agent-based model (CN-ABM) to simulate on-campus disease transmission scenarios at the micro-scale. The CN-ABM establishes a contact network for each agent based on their daily activity pattern, evaluates the agent's health status change in different activity environments, and then simulates the epidemic curve on campus. Based on the developed model, we identify how different community risk levels, teaching modalities, and vaccination rates would shape the epidemic curve.

Results: The results show that in scenarios where vaccination is not available, restricting on-campus students to under 50% can largely flatten the epi curve (peak value < 2%); and the best result (peak value < 1%) can be achieved by limiting on-campus students to less than 25%. In scenarios where vaccination is available, it is suggested to maintain a maximum of 75% on-campus students and a vaccination rate of at least 45% to suppress the curve (peak value < 2%); and the best result (peak value < 1%) can be achieved at a vaccination rate of 65%. The study also derives the transmission chain of infectious agents, which can be used to identify high-risk activity environments.

Conclusions: The developed CN-ABM model can be employed to evaluate the health outcome of COVID-19 outbreaks on campus based on different disease transmission scenarios. It can assist local government and school officials with developing proactive intervention strategies to safely reopen schools.

1. Background

School environments are characterized by frequent social gatherings and extensive interpersonal interactions, making them ideal breeding grounds for viruses [1, 2]. Due to the highly contagious nature of the coronavirus disease 2019 (COVID-19), school closure and pedagogical transitions were widely implemented to control the spread of the disease [3]. The World Health Organization (WHO) estimated that about 90 percent of the world’s students, which were more than 1.5 billion children and young adults, were affected by school closure [4]. The cascading impacts of school closure included reduced work efficiency [5], lack of educational resources [6], and mental health issues caused by social isolation [7]. Burdened with these grave concerns and the political pressure to revive the economy, governments of many countries laid out plans to reopen schools. However, these reopening plans and their implementation often lacked scientific evidence to weigh the potential health consequences. For example, a national survey of more than 1,500 universities and colleges in the United States revealed over 51,000 COVID-19 cases and 60 deaths as a result of school reopening in early September 2020 [8]. The sobering

reality signifies that it is of utmost significance to employ rigorous measures to evaluate the health risk for school reopening [9].

Existing studies have used process-based dynamic epidemic models, primarily the Susceptible-Exposed-Infective-Recovered (SEIR) model and its variations, to simulate the potential for COVID-19 outbreaks [10–13]. Although these models can project the epidemic development under different social distancing scenarios, they cannot be easily implemented in a school environment without major modification. First, existing studies are mainly focused on macro-scale assessments with aggregate administrative units (e.g., counties, census tracts). They are unable to model the intricacy of the disease transmission process at the individual scale, known as the micro-scale, which plays a vital role in determining the likelihood of virus spread in a school environment. Second, existing studies mostly employ deterministic models without considering the stochastic transmission process, such as the infection rates in different activity environments (e.g., inside buildings, outdoor); and these uncertainties at the micro-scale can dictate the likelihood of outbreaks when school reopens. To date, existing micro-scale predictive models, especially those applicable to schools, are considerably lacking.

In this paper, we propose a contact network agent-based model (CN-ABM) to simulate the COVID-19 transmission process in a school environment. In the model, we define on-campus students as agents and construct a fine-grained dynamic contact network between agents based on their daily activity patterns and movement trajectories. Then, we employ the model to simulate on-campus transmission scenarios under WHO's guidelines for school reopening [14]. Specifically, we evaluate how the epidemic curve (i.e., epi curve) is shaped by different community risk levels, teaching modalities, and vaccination rates. It is hoped that the proposed model can help project timelines to safely reopen school amid the ongoing COVID-19 vaccination practices.

The paper is organized as follows. Section 2 introduces the methods, including the conceptual framework and the proposed simulation model. Section 3 applies the model to a school environment and derives the results, including the epi curve and the transmission chain. Section 4 performs the sensitivity analysis of the model by incorporating the vaccination rate, discusses its public health implications, and also presents the limitations. Finally, Sect. 5 concludes the study with future directions.

2. Methods

2.1 Conceptualizing contact network

The agent-based model (ABM) is a micro-scale model that simulates the synchronous interactions of agents based on pre-defined rules [15]. The ABM has been integrated into network science to enhance our understanding of human behaviors [16]. In a network-based ABM, each agent can be represented as a node, which interacts with other agents under predefined behavioral assumptions in an abstracted interaction network [17]. Recently, the network-based ABM has received elevated attention in near real-

time genome sequencing of the SARS-CoV-2 virus [18]. Its applications to the COVID-19 transmission in communities (e.g., schools) are relatively lacking.

The transmission process of the SARS-CoV-2 virus can be regarded as the transition of an individual's health status via interactions with infectious agents [19]. This process can be illustrated by Fig. 1, where an agent's health status could change if the agent's contact network entails an infectious agent. Additionally, the internal transmission process inside a school can be influenced by the community spread beyond the school environment [20]. We thus incorporate the community risk as an external node into the contact network, meaning that each agent can become infectious at a given probability even without contacting other internal agents (Fig. 1).

To construct the contact network, all agents' daily activity patterns, including their movement trajectories, locations of stay in an activity environment (e.g., dining hall, residential building), and periods of stay, must be acquired. Deriving these activity patterns for all agents is a prerequisite for building the contact network at each time point. This process in our case study is detailed in the Appendix.

2.2 Infection phases

Based on the classical SEIR model, an agent's health status in an infection cycle can be divided into four statuses: susceptible (S), exposed (E), infectious (I), and recovered (R). The transition of the health status, reflecting the disease progression, is key to simulating the spread of an epidemic. Based on the study of modeling school reopening [21] and the successive vaccination stage [22], we introduce six heath statuses to illustrate a complete infection cycle, including susceptible (S), exposed (E), pre-symptomatic (I_p), infected (I), recovered/removed (R), and vaccinated (V). These six health statuses constitute five infection phases, as shown in Fig. 2.

The transition of an agent's health status at each infection phase is articulated below.

Phase 1 (S → E): the probability of an agent transitioning from S to E in an activity environment *j* at time *t* is $P_{t,j}$. It is dependent on both the internal infection probability $\Phi_{t,j}$ and the external (community) infection probability Ψ, as shown in Eq. (1). An agent's internal infection probability $\Phi_{t,j}$ in activity environment *j* at time t is shown in Eq. (2). An agent's external infection Ψ is a ratio of the community infection rate p_c to the agent's health level *H*, as shown in Eq. (3)

$$P_{t,j} = 1 - (1 - \Phi_{t,j})(1 - \Psi) \quad (1)$$

$$\Phi_{t,j} = \frac{1 - (1 - Kp_j)^{m_t}(1 - p_j)^{n_t}}{H} \quad (2)$$

$$\Psi = \frac{p_c}{H} \quad (3)$$

Notation:

H: agent's health level;

K: decay coefficient for the infection rate of an I_p-status agent;

m_t: number of I_p-status neighbors in an agent's contact network at time t;

n_t: number of I-status neighbors in an agent's contact network at time t;

p_c: community infection rate;

p_j: infection rate in activity environment j;

$P_{t,j}$: probability of an agent transitioning from S to E in activity environment j at time t;

$\Phi_{t,j}$: internal infection probability;

Ψ: external infection probability.

Phase 2 ($E \rightarrow I_p$): an E-status agent transitions to the I_p-status after a latent period (ε^{-1}). During this phase (t through $t+\varepsilon^{-1}$), the agent is not infectious.

Phase 3 ($I_p \rightarrow I$): an I_p-status agent transitions to the I status after the prodromal period (μ_p^{-1}); and the duration from E to I is the incubation period σ^{-1}. During this phase ($t+\varepsilon^{-1}$ through $t+\sigma^{-1}$), an I_p-status agent infects all S-status neighbors at an infection rate Kp_j if they are within the same contact network.

Phase 4 ($I \rightarrow R$): an I-status agent transitions to R-status after the infection period (γ^{-1}). During this phase ($t+\sigma^{-1}$ through $t+\varepsilon^{-1}+\gamma^{-1}$), the I-status agent infects S-status neighbors in its contact network at the infection rate p_j.

Phase 5 ($S \rightarrow V$): an S-status agent transitions to V-status, if it is vaccinated. A V-status agent is not infectious and cannot be infected. The number of S-status agents is determined by the initial number of S-status agents S_0 and the immunized agents $\alpha v S_0$, where v is the vaccination rate and α is the vaccine efficacy [23], as is shown in Eq. (4).

$$S = (1 - \alpha v)S_0 \quad (4)$$

The parameters in Fig. 2 and Equations (1) through (4) are derived from existing epidemiological parameters, as shown in Table 1.

Table 1
Epidemiological parameters used in the simulation model.

Parameter	Explanation	Value	Reference
σ^{-1}	Incubation period	$\sigma^{-1} \sim$ lognormal (1.6, 0.5)$\cap\sigma^{-1}\in$[2, 14] days	[24]
$\mu_p{}^{-1}$	Prodromal period	2 days	[25]
ε^{-1}	Latent period	σ^{-1} - $\mu_p{}^{-1}$	-
γ^{-1}	Infection period	$\gamma^{-1} \sim$ lognormal (2.05, 0.25)	[26]
K	Decay coefficient for the infection rate of an I_p-status agent	1/3	[27]
p_j	Internal infection rate in an activity environment j	Dining hall: 3.03e^{-4}/min; residential building: 1.74e^{-4}/min; lecture hall (including library): 3.30e^{-5}/min	[27]
p_c	Community infection rate	9.5e^{-8}/min	[20]
H	Agent's health level	$1/H \sim$ normal(1, 0.1)	[28]
α	Vaccine efficacy	80%	[29]

The workflow for the ABM simulation is given in Fig. 3. We call this proposed model the contact network agent-based model (CN-ABM).

3. Results

Following the aforementioned method, we built the proposed CN-ABM model in MATLAB R2019a. The code of the model can be access in GitHub (https://github.com/xic19022/cnabm). Our computational environment was as follows: CPU Intel(R) Xeon(R) E5-2620 (8-core/2.10GHz) and RAM of 64GB. We then applied the model in a real-world school environment with different environmental settings.

3.1 Model initialization

Our study area was a university campus located in Southern China. We derived the building footprints and the road networks on campus using the Baidu Map application programming interface (API) (https://lbsyun.baidu.com/), as shown in Fig. 4. The shortest network distance between every two buildings was also derived by the API and was converted to walking time (in minutes) based on the

average human walking speed (i.e., 5 km per hour). To initialize the simulation, we generated 10,000 agents in the starting scenario ($t = 0$) and introduced 1‰ pre-symptomatic cases among them. We allocated these agents into the residential buildings proportional to the building capacities. Then, each agent was assumed to follow a similar activity pattern but select the activity location of the same type randomly. The details about generating the agents' activity patterns are given in the Appendix.

In the first set of analyses, we consider twelve school reopening scenarios based on different teaching modalities (i.e., the composition of on-campus and distance-learning students) and community risk levels (i.e., the community infection rate), as shown in Table 2. We consider that the distance-learning students were not present on campus and were thus excluded from the simulation. We did not consider the vaccination phase (i.e., Phase 5 in Fig. 2) in the initial set of analyses, as it is discussed in the follow-up section. For each scenario, we performed the simulation for twenty-five weeks at a one-minute timestamp; we also repeated each simulation five times to account for the stochastic nature of the disease transmission.

Table 2
Twelve school reopening scenarios based on different community risk levels and teaching modalities.

	Student composition (% of distance-learning)			
Community risk level (community infection rate)	In-class (0%)	Mostly in-class (25%)	Hybrid (50%)	Mostly online (75%)
No risk (0)	N-S0	N-S25	N-S50	N-S75
Low risk (p_c)*	L-S0	L-S25	L-S50	L-S75
High risk (5x p_c)	H-S0	H-S25	H-S50	H-S75
*The community infection rate p_c is $9.5e^{-8}$/min [20].				

3.2 Simulated epi curves

The simulation results in terms of the epi curves (i.e., the percentage of active infectious agents over time) under the twelve school reopening scenarios are given in Fig. 5. Figure 5 reveals two important epidemic patterns. First, the teaching modality largely affects the epi curve. For example, on a low community risk level when all students are on campus (L-S0), the peak value of the epi curve or the maximum percentage of infections is 22.38% (the blue curve, Fig. 5b). Then, reducing the on-campus students by 25% (L-S25), 50% (L-S50), and 75% (L-S75) will considerably flatten the epi curve, where the peak values are 12.40%, 1.64%, and 0.40%, respectively (Fig. 5b). Second, the influence of the community risk on the transmission is moderate, and a high community risk advances the emergence of the peak time. For example, under the same modality of "mostly in-class (red curves in Fig. 5)" but different

community risk levels, the peaks of the epi curves emerge on the 95th day (N-S25, no risk, Fig. 5a), the 83rd day (L-S25, low risk, Fig. 5b), and the 64th day (H-S25, high risk, Fig. 5c), respectively. The statistics of the epi curves, including the peak height and the peak day, are given in Table 3.

Table 3
Statistics of the simulation results under school reopening scenarios in Table 2.

Scenario	Peak height (min, max)*	Peak reduction rate**	Peak day (min, max)*
N-S0	21.49% (21.30%, 22.02%)	-	74.49 (66.54, 74.66)
N-S25	12.03% (11.29%, 12.40%)	44.02%	94.61 (83.81, 96.24)
N-S50	0.14% (0.12%, 0.36%)	99.35%	10.53 (8.07, 159.98)***
N-S75	0.12% (0.12%, 0.16%)	99.44%	6.38 (5.27, 8.35)***
L-S0	22.38% (21.18%, 23.77%)	-	64.91 (60.44, 67.21)
L-S25	12.40% (11.60%, 13.23%)	44.59%	82.93 (78.30, 86.56)
L-S50	1.64% (1.56%, 2.02%)	92.67%	124.93 (121.58, 144.74)
L-S75	0.40% (0.32%, 0.48%)	98.21%	146.17 (111.33, 168.63)
H-S0	23.38% (22.66%, 24.46%)	-	53.26 (52.40, 55.18)
H-S25	13.52% (13.41%, 14.11%)	42.17%	63.64 (62.96, 69.87)
H-S50	3.64% (3.10%, 4.00%)	84.43%	73.54 (63.37, 90.77)
H-S75	1.12% (0.92%, 1.16%)	95.21%	151.72 (100.54, 165.57)
*The values of the peak height and peak day are derived from the median of the five repeated simulations for each scenario.			
**Defined as the current peak height relative to the peak height in the corresponding baseline scenario (S0).			
***In this scenario, the peak emerges early, as the outbreak is not prominent.			

3.3 Transmission chain

The proposed CN-ABM model is capable to project the COVID-19 epi curve for a potential outbreak scenario. More importantly, it can be used to infer the timeline of the disease progression, such as the transmission chain. Figure 6 illustrates an example of the inferred transmission chain for an infectious agent (i.e., the initial case) over the first 35 days of the disease progression. Specifically, the figure shows that under the N-S0 scenario, the initial case can affect 104 other agents in its contact network, while most of the infections (58.65%) occur in a residential building (i.e., 61 agents in the residential building, 30 agents in the dining hall, 12 agents in the lecture hall, and 1 agent in the library). Constructing this

transmission chain can help track where and when the transmission takes place and can provide evidence to formulate proactive intervention strategies in high-risk activity environments [30].

4. Discussion

4.1 How does vaccination shape the epi curve?

While phases of vaccination are rolling out in most world regions, there has been a lack of understanding about how the vaccination shapes the epi curve at the community scale [23]. In the second set of analyses, we evaluated the health outcomes under fifteen school reopening scenarios based on combinations of community risk levels and vaccination rates (Table 4). The vaccination phase (i.e., Phase 5 in Fig. 2) presumes that when a portion of S-status agents convert to V-status, they become immune to the virus and are excluded from the infection cycle. To facilitate the bi-variate analysis, we assumed all agents were in-class (0% distance-learning) in the model initialization. The simulation results in terms of the epi curves are given in Fig. 7.

Table 4
Fifteen school reopening scenarios based on different community risk levels and vaccination rates.

Community risk level	**Vaccination rate (% of vaccinated agents)**				
(community infection rate)	**5%**	**25%**	**45%**	**65%**	**85%**
No risk (0)	N-V5	N-V25	N-V45	N-V65	N-V85
Low risk (p_c)*	L-V5	L-V25	L-V45	L-V65	L-V85
High risk (5x p_c)	H-V5	H-V25	H-V45	H-V65	H-V85
*The community infection rate p_c is $9.5e^{-8}$/min [20].					

Figure 7 reveals two important epidemic patterns. First, the vaccination rate is the primary parameter shaping the epi curve. For example, on a low community risk level, high vaccination rates will largely flatten the curve—the vaccination rates of 5% (L-V5), 25% (L-V25), 45% (L-V45), 65% (L-V65), and 85% (L-85) yield a peak value of 19.62%, 11.73%, 5.23%, 1.14%, and 0.20%, respectively (Fig. 7b). Second, similar to the results in Sect. 3.2, the influence of the community risk is moderate, and a high community risk slightly advances the emergence of the peak. For example, at the vaccination rate of 45% (the green curves in Fig. 7), the peak of the epi curve emerges on the 102nd day (N-V45, no risk, Fig. 7a), the 90th day (L-V45, low-risk, Fig. 7b), and the 71st day (H-V45, high risk, Fig. 7c), respectively.

Our third set of analyses simulates the health outcome as a result of different teaching modalities and vaccination rates. Since the distance-learning modality and vaccination are both preventive measures to

contain the disease transmission, it is expected that combining these two measures will mitigate the likelihood of outbreaks to the largest extent. Thus, we designed twenty school reopening scenarios by combining different teaching modalities and vaccination rates (Table 5), whereas all scenarios are predicated on a low community risk level (p_c = 9.5e^{-8}/min). The simulation results in terms of the epi curves are given in Fig. 8.

Figure 8 shows that when 50% (Fig. 8c) or 75% (Fig. 8d) of the students are off-campus, the virus spread will be well controlled. While in reality, it is not likely to maintain a high rate of distancing learning modality over an elongated period, the result further suggests that a modest vaccination rate will also help to curb the infection when most students return to campus. Specifically, when 75% of the students are on campus, a vaccination rate of 45% or above can effectively flatten the curve by limiting its peak value to under 2% (the green curve in Fig. 8b); and the best result (peak value < 1%) can be achieved when the vaccination rate is above 65% (the purple curve in Fig. 8b). This result indicates that social distancing interventions, such as hybrid teaching modalities, can be cautiously relieved when a critical threshold of the vaccination rate is reached.

The statistics of the epi curves in Fig. 7 and Fig. 8 are given in the Appendix.

Table 5
Twenty school reopening scenarios based on different teaching modalities and vaccination rates.

Student composition (% of distance-learning)	**Vaccination rate**				
	5%	**25%**	**45%**	**65%**	**85%**
In-class (0%)	S0-V5	S0-V25	S0-V45	S0-V65	S0-V85
Mostly in-class (25%)	S25-V5	S25-V25	S25-V45	S25-V65	S25-V85
Hybrid (50%)	S50-V5	S50-V25	S50-V45	S50-V65	S50-V85
Mostly online (75%)	S75-V5	S75-V25	S75-V45	S75-V65	S75-V85

4.2 Public health implications

The proposed CN-ABM model and its application for school reopening scenarios are among the first to model the COVID-19 infection at the micro-scale. By running the model under different community risk levels, teaching modalities, and vaccination rates, we can glean practical implications for school's reopening plans in response to the evolving epidemic situations.

First, micro-scale modeling and simulations are of critical significance for uncovering the pandemic's development mechanism and potential health outcomes. Existing COVID-19 modeling work largely utilizes macro-scale models to simulate variables and trends of disease development, such as daily

cases of infection (e.g.[10]). These studies were mostly implemented for a large region (e.g., country, state) with the smallest analysis unit being an administrative unit (e.g., county, town). Such macro-scale modeling is not able to account for the uncertainties in the transmission process, such as individual attributes, activity patterns, activity environments, and interpersonal interactions. The proposed CN-ABM model, on the contrary, takes a bottom-up approach to construct the transmission mechanism on the individual level at refined spatiotemporal scales. This attempt is necessary as the implementation of preventive measures, such as social distancing, is mostly oriented towards individuals [31]. In addition, the CN-ABM model can generate the transmission chain of an infectious agent, which helps to identify high-risk activity environments for proactive interventions.

Second, as the CN-ABM model is built on three guiding metrics (i.e., community risk level, teaching modality, and vaccination rate), it can provide quantifiable assessment results to evaluate the effectiveness and consequences of different school reopening plans. Specifically, our three sets of analyses suggest practical school reopening strategies to minimize potential health adversities in a general scenario (i.e., low community risk): (1) in scenarios where vaccination is not available, it is suggested to restrict on-campus students to under 50%, as it can largely flatten the epi curve (peak value < 2%, the green curve in Fig. 5b); and the best result (peak value < 1%) can be achieved by limiting on-campus students to < 25% (the purple curve in Fig. 5b). (2) In scenarios where vaccination is available, it is suggested to maintain < 75% on-campus students and a vaccination rate of > 45% to suppress the epi curve (peak value < 2%, the green curve in Fig. 8b); and the best result (peak value < 1%) can be achieved at a vaccination rate of > 65% (the purple curve in Fig. 8b).

The study is not without limitations. First, some of the epidemiological parameters used in the model, such as the infection rate and vaccine effectiveness, were solicited from the literature. In reality, tiers of uncertainties, such as the room capacity and disinfection levels, can dictate the infection rate. Also, in many countries, such as the United States, the active infection rate is not published due to the enforcement of health data regulations, such as the Health Insurance Portability and Accountability Act [32]. Future research should investigate the variation and temporality of these epidemiological parameters with clinical evidence in a study area [33]. Second, our model initialization was based on predefined activity patterns by applying a stochastic selection approach. Thus, the simulation results provide only general criteria for school reopening and may not accommodate the needs of every educational institution, where the student enrollment, teaching modalities, course schedules, and social distancing policies vary considerably. Future implementation of the model should incorporate real-world mobility data (e.g., travel diaries, GPS trajectories) and local social distancing policies to improve the applicability of the model.

5. Conclusions

While phases of COVID-19 vaccination are rolling out, amid the need to revive the economy, it is essential to reopen schools safely while minimizing potential health adversities. Although levels of policy guidance to initiate the school reopening are underway, many of these recommendations lack scenario-based

evaluations. Under this context, the proposed CN-ABM model can provide scientific evidence to corroborate the preventive measures and public policies for school reopening. The scenario-based assessments can help government stakeholders and school administrators understand the joint effects of the community risk level, teaching modality, and vaccination rate on shaping the epi curve. Findings in this paper can further contribute to strategic decision-making that weighs the timing of school reopening against the projected health consequences. It also complements the lack of micro-scale study on COVID-19 and can be extended to other community settings, such as residential neighborhoods, workplaces, and shopping malls, and can eventually contribute to developing proactive health intervention strategies in these settings.

Abbreviations

ABM: agent-based model;

API: application programming interface;

CN-ABM: contact network agent-based model;

COVID-19: coronavirus disease 2019;

SEIR: Susceptible-Exposed-Infective-Recovered;

WHO: World Health Organization

Declarations

Ethics approval and consent to participate

Not applicable.

Consent for publication

Not applicable.

Availability of data and materials

The data and codes for this study can be accessed in GitHub (https://github.com/xic19022/cnabm).

Competing interests

The authors declare that they have no competing interests.

Funding

This research was supported by the National Natural Science Foundation of China (Grant No. 41971372), in part by the Natural Science Foundation of Guangdong Province (Grant No. 2020A1515010680).

Authors' contributions

CL contributed towards conceptualization, methodology, and writing the initial draft. XC and LZ contributed towards conceptualization and revising the draft. YL and HT contributed towards revising the draft. All authors read and approved the manuscript.

Acknowledgements

Not applicable.

References

1. Chao DL, Halloran ME, Longini IJ: **School opening dates predict pandemic influenza A(H1N1) outbreaks in the United States**. *J INFECT DIS* 2010, **202**(6):877-880.
2. Gog JR, Ballesteros S, Viboud C, Simonsen L, Bjornstad ON, Shaman J, Chao DL, Khan F, Grenfell BT: **Spatial Transmission of 2009 Pandemic Influenza in the US**. *PLOS COMPUT BIOL* 2014, **10**(6):e1003635.
3. Viner RM, Russell SJ, Croker H, Packer J, Ward J, Stansfield C, Mytton O, Bonell C, Booy R: **School closure and management practices during coronavirus outbreaks including COVID-19: a rapid systematic review**. *Lancet Child Adolesc Health* 2020, **4**(5):397-404.
4. WHO: **Coronavirus disease (COVID-19). Situation report - 77**. In.; 2020. [cited April 6, 2020]. https://www.who.int/docs/default-source/coronaviruse/situation-reports/20200406-sitrep-77-covid-19.pdf?sfvrsn=21d1e632_2
5. Li X, Xu W, Dozier M, He Y, Kirolos A, Theodoratou E: **The role of children in transmission of SARS-CoV-2: A rapid review**. *J GLOB HEALTH* 2020, **10**(1):11101.
6. UNESCO: **Educational applications and platforms to mitigate impact of COVID-19 school closures**. In.; 2020. [cited March 9, 2020]. https://en.unesco.org/themes/education-emergencies/coronavirus-school-closures/solutions
7. Brooks SK, Webster RK, Smith LE, Woodland L, Wessely S, Greenberg N, Rubin GJ: **The psychological impact of quarantine and how to reduce it: rapid review of the evidence**. *The Lancet* 2020, **395**(10227):912-920.
8. Cai W: **Tracking coronavirus cases at US colleges and universities**. *The New York Times* 2020, **25**. [cited September 3, 2020]. https://www.nytimes.com/interactive/2020/us/covid-college-cases-tracker.html
9. Mallapaty S: **How schools can reopen safely during the pandemic**. *NATURE* 2020, **584**(7822):503-504.

10. Chen X, Zhang A, Wang H, Gallaher A, Zhu X: **Compliance and containment in social distancing: mathematical modeling of COVID-19 across townships**. *International journal of geographical information science: IJGIS* 2021, **35**(3):446-465.
11. Read JM, Bridgen JR, Cummings DA, Ho A, Jewell CP: **Novel coronavirus 2019-nCoV: early estimation of epidemiological parameters and epidemic predictions**. *MedRxiv* 2020.
12. Wu JT, Leung K, Leung GM: **Nowcasting and forecasting the potential domestic and international spread of the 2019-nCoV outbreak originating in Wuhan, China: a modelling study**. *The Lancet* 2020, **395**(10225):689-697.
13. Zeng T, Zhang Y, Li Z, Liu X, Qiu B: **Predictions of 2019-nCoV Transmission Ending via Comprehensive Methods**. *arXiv preprint arXiv:2002.04945* 2020.
14. WHO: **Considerations for school-related public health measures in the context of COVID-19**. In.; 2020. [cited September 14,2020]. https://www.who.int/publications/i/item/considerations-for-school-related-public-health-measures-in-the-context-of-covid-19
15. Wooldridge M: **An introduction to multiagent systems**: John wiley & sons; 2009.
16. Chen X, Kwan M, Li Q, Chen J: **A model for evacuation risk assessment with consideration of pre- and post-disaster factors**. *Computers, environment and urban systems* 2012, **36**(3):207-217.
17. Cardinot M, O Riordan C, Griffith J, Perc M: **Evoplex: A platform for agent-based modeling on networks**. *SoftwareX* 2019, **9**:199-204.
18. Rockett RJ, Arnott A, Lam C, Sadsad R, Timms V, Gray K, Eden J: **Revealing COVID-19 transmission in Australia by SARS-CoV-2 genome sequencing and agent-based modeling**. *NAT MED* 2020, **26**(9):1398-1404.
19. Chang SL, Harding N, Zachreson C, Cliff OM, Prokopenko M: **Modelling transmission and control of the COVID-19 pandemic in Australia**. *NAT COMMUN* 2020, **11**(1):5710.
20. Gemmetto V, Barrat A, Cattuto C: **Mitigation of infectious disease at school: targeted class closure vs school closure**. *BMC INFECT DIS* 2014, **14**:695.
21. Di Domenico L, Pullano G, Sabbatini CE, Boëlle P, Colizza V: **Modelling safe protocols for reopening schools during the COVID-19 pandemic in France**. *NAT COMMUN* 2021, **12**(1):1073.
22. Huang B, Wang J, Cai J, Yao S, Chan PKS, Tam TH, Hong Y, Ruktanonchai CW, Carioli A, Floyd JR *et al*: **Integrated vaccination and physical distancing interventions to prevent future COVID-19 waves in Chinese cities**. *Nature human behaviour* 2021.
23. Kim JH, Marks F, Clemens JD: **Looking beyond COVID-19 vaccine phase 3 trials**. *NAT MED* 2021, **27**(2):205-211.
24. McAloon C, Collins A, Hunt K, Barber A, Byrne AW, Butler F, Casey M, Griffin J, Lane E, McEvoy D *et al*: **Incubation period of COVID-19: a rapid systematic review and meta-analysis of observational research**. *BMJ OPEN* 2020, **10**(8):e39652.
25. Kim SE, Jeong HS, Yu Y, Shin SU, Kim S, Oh TH, Kim UJ, Kang SJ, Jang HC, Jung SI *et al*: **Viral kinetics of SARS-CoV-2 in asymptomatic carriers and presymptomatic patients**. *INT J INFECT DIS*

2020, **95**:441-443.

26. Wolfel R, Corman VM, Guggemos W, Seilmaier M, Zange S, Muller MA, Niemeyer D, Jones TC, Vollmar P, Rothe C *et al*: **Virological assessment of hospitalized patients with COVID-2019 (vol 581, pg 465, 2020)**. *NATURE* 2020, **588**(7839):E35.
27. Chen Y, Wang A, Yi B, Ding K, Wang H, Wang J, Shi H, Wang S, Xu G: **The epidemiological characteristics of infection in close contacts of COVID-19 in Ningbo city**. *Chin J Epidemiol* 2020, **41**(5):668-672.
28. Yang Y, Atkinson PM: **Individual Space-Time Activity-Based Model: A Model for the Simulation of Airborne Infectious-Disease Transmission by Activity-Bundle Simulation**. *Environment and Planning B: Planning and Design* 2008, **35**(1):80-99.
29. WHO: **WHO lists additional COVID-19 vaccine for emergency use and issues interim policy recommendations**. In.; 2021. [cited May 7, 2021]. https://www.who.int/news/item/07-05-2021-who-lists-additional-covid-19-vaccine-for-emergency-use-and-issues-interim-policy-recommendations
30. Kelvin AA, Halperin S: **COVID-19 in children: the link in the transmission chain**. *The Lancet infectious diseases* 2020, **20**(6):633-634.
31. Gostin LO, Wiley LF: **Governmental Public Health Powers During the COVID-19 Pandemic: Stay-at-home Orders, Business Closures, and Travel Restrictions**. *JAMA : the journal of the American Medical Association* 2020, **323**(21):2137-2138.
32. Edemekong P, Annamaraju P, Haydel M: **Health Insurance Portability and Accountability Act**. *StatPearls* 2020.
33. Corum J, Grady D, Wee S, Zimmer C: **Coronavirus vaccine tracker**. *The New York Times* 2020, **5**. [cited February 5, 2021]. https://www.nytimes.com/interactive/2020/science/coronavirus-vaccine-tracker.html

Figures

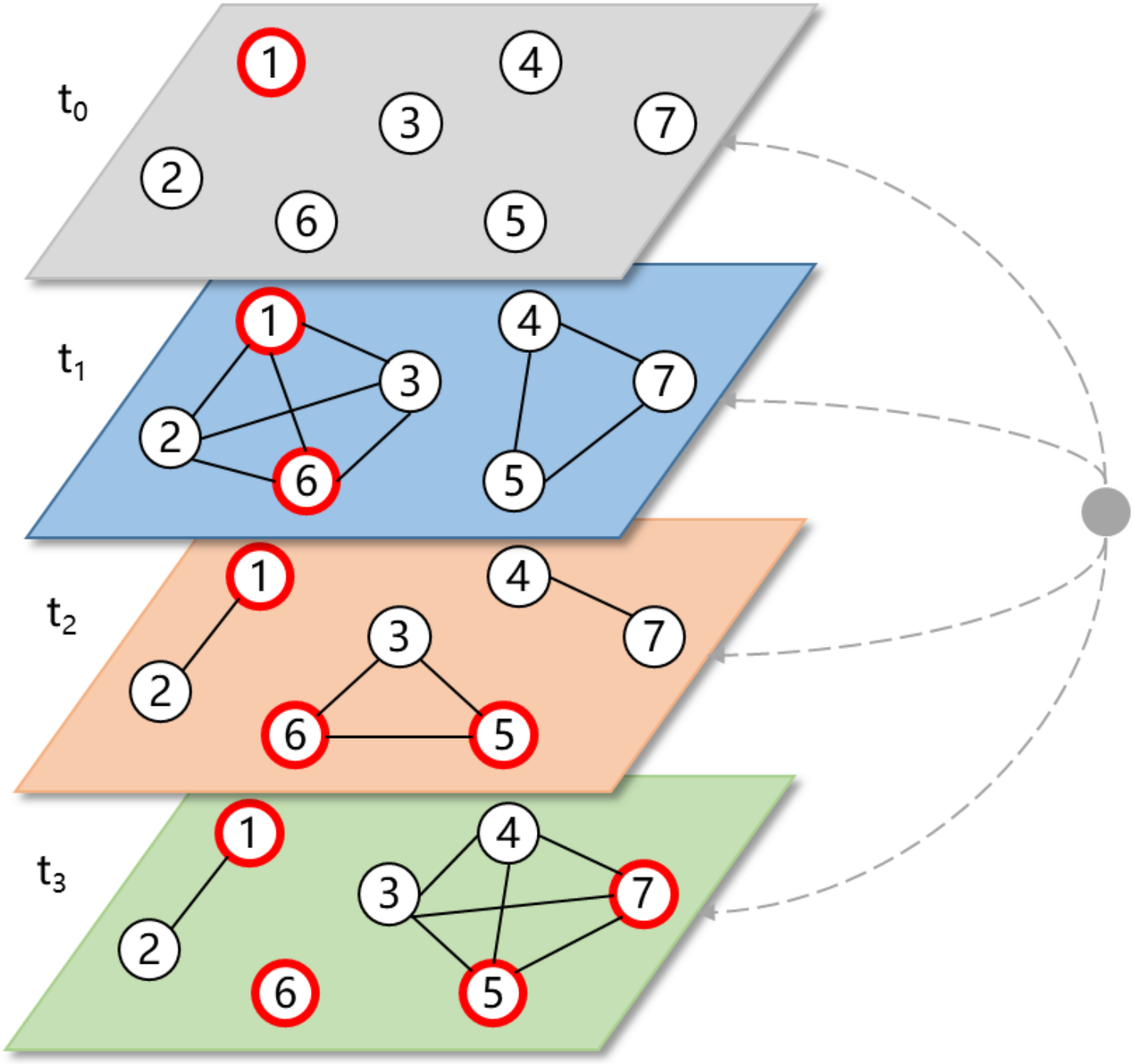

Figure 1

Schematic illustration of the contact network. Red nodes are infectious agents; lines are interactions between agents via their close contact at a time point. An external node is introduced to represent the community risk.

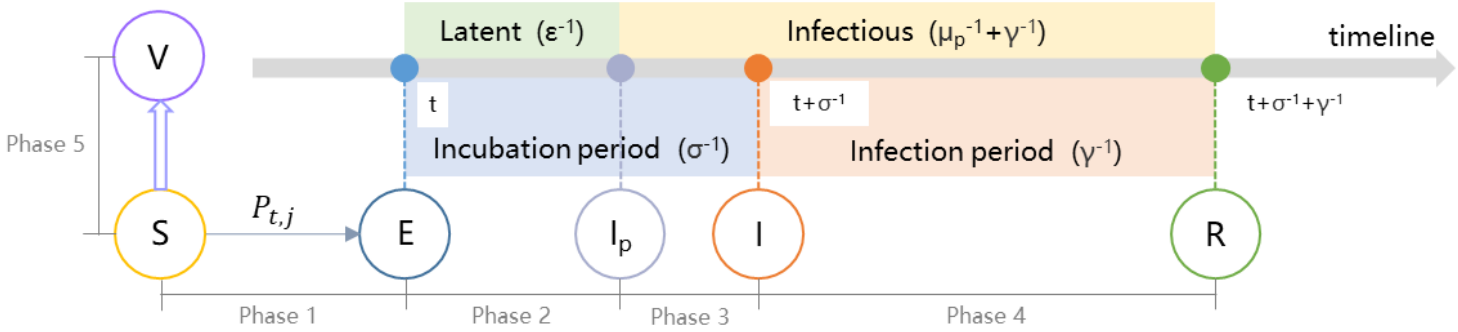

Figure 2

Schematic illustration of an infection cycle with the change of an agent's health status (E = exposed, Ip = pre-symptomatic, I = infected, R = recovered, and V = vaccinated).

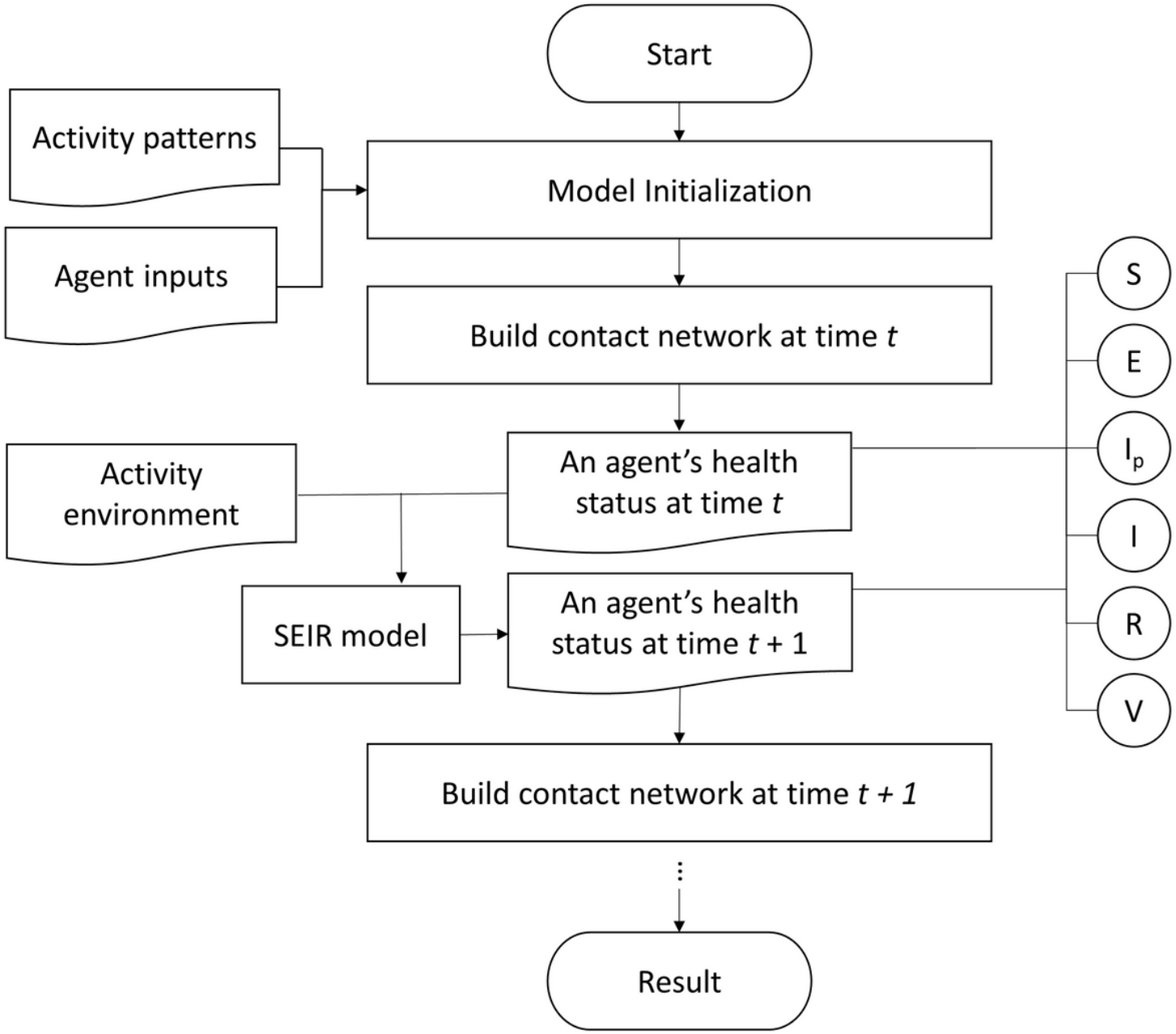

Figure 3

Workflow of the CN-ABM model for simulating COVID-19 transmission in a school environment.

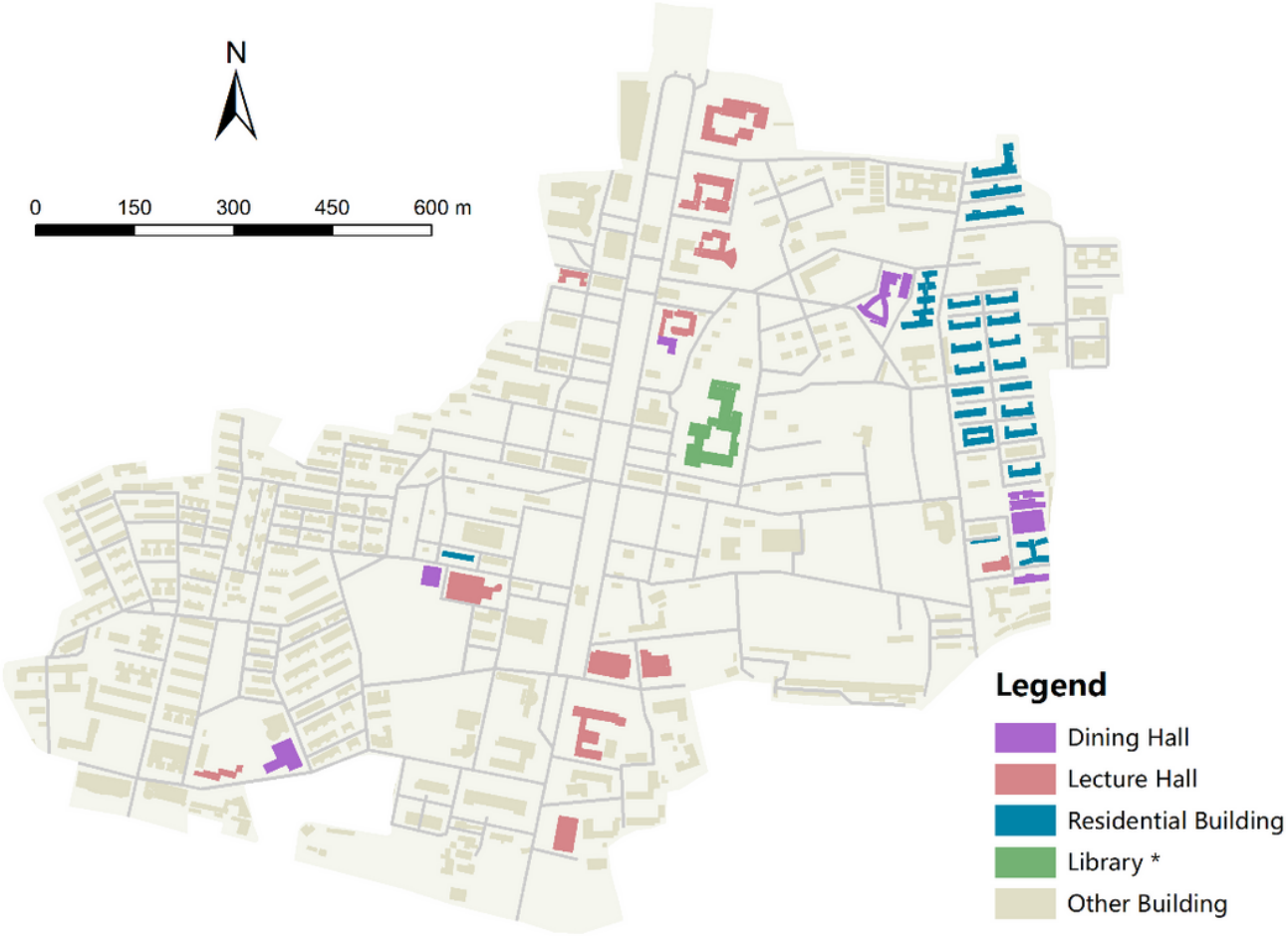

Figure 4

Building footprints of the campus in the study area. *The library is considered a lecture hall in the model simulation; other buildings (e.g., administrative buildings) are excluded from the simulation.

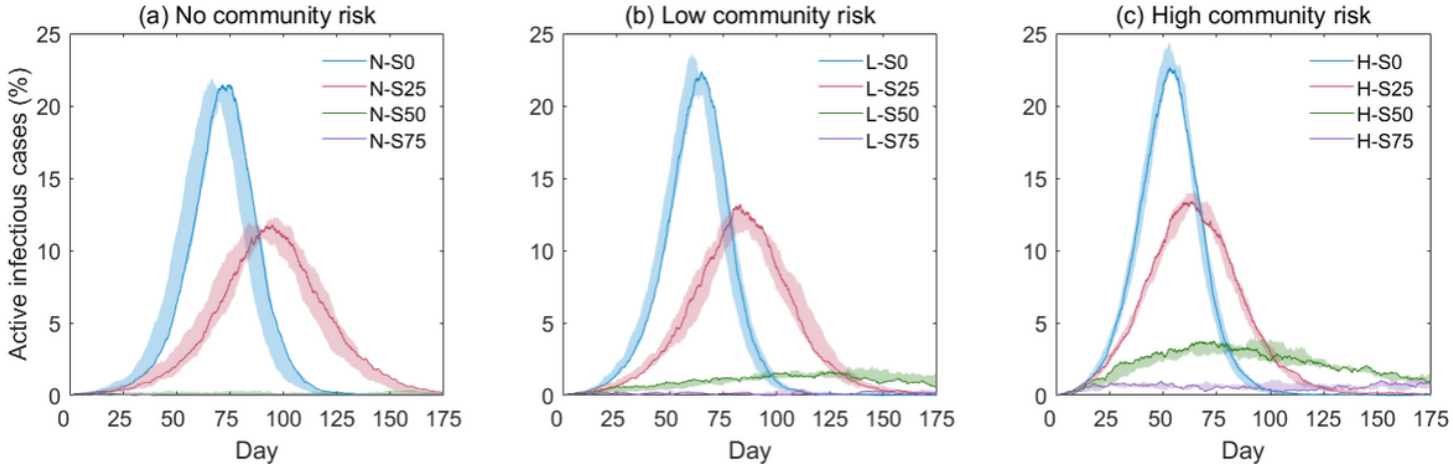

Figure 5

Simulation results under different school reopening scenarios at different community risks: (a) no risk, (b) low risk, and (c) high risk. Curves in different colors represent different teaching modalities; the vertical axis (Y) is the simulated active infectious cases as a percentage of the total agents (%); the horizontal axis (X) is the day of simulation.

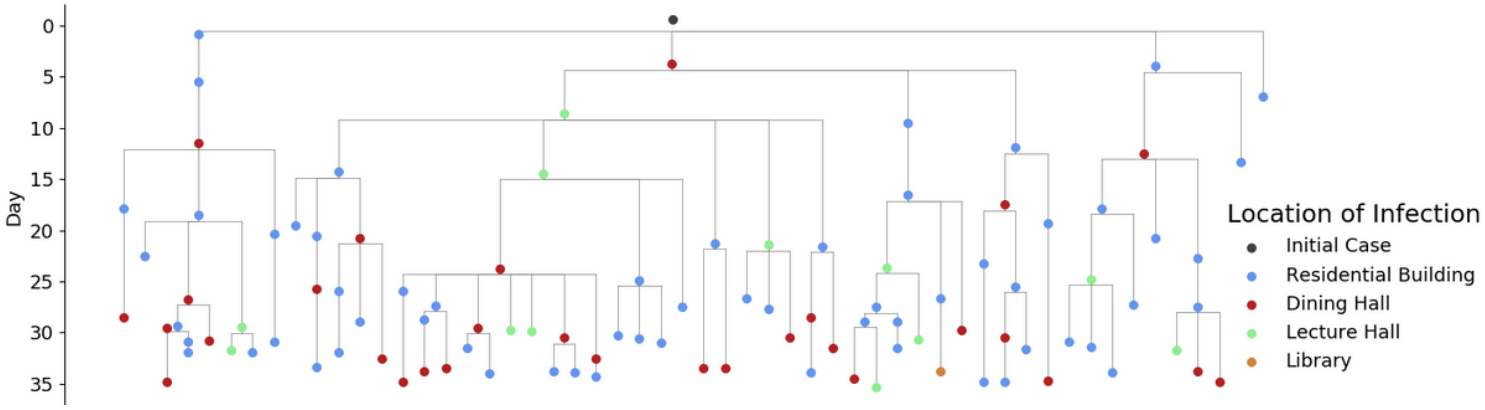

Figure 6

The transmission chain of an agent in the first 35 days of the disease progression under the N-S0 scenario.

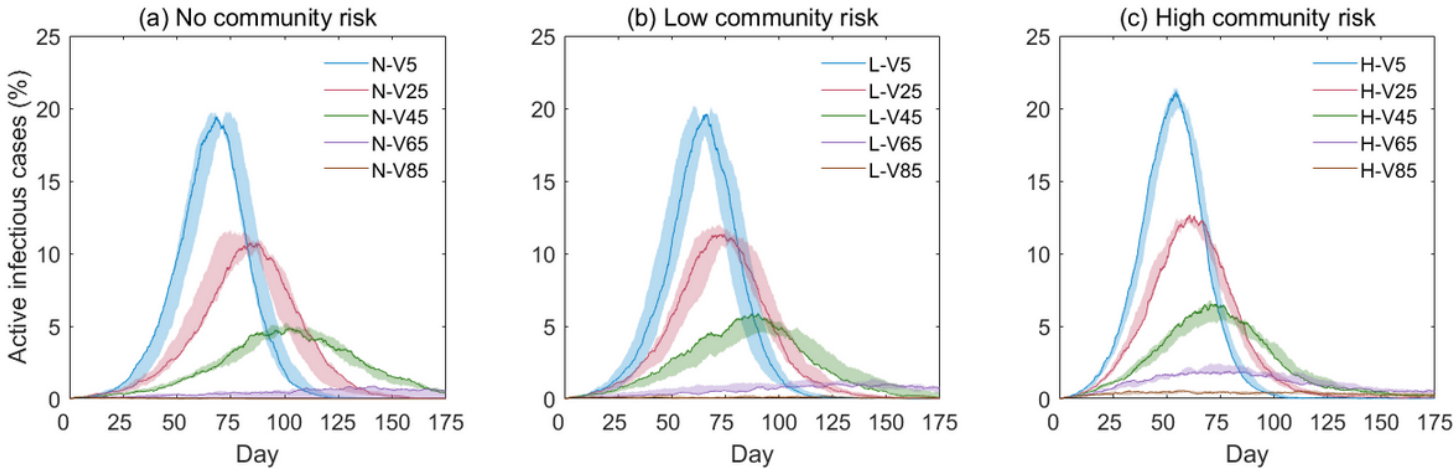

Figure 7

Simulation results under different school reopening scenarios at different community risks: (a) no risk, (b) low risk, and (c) high risk. Curves in different colors represent different vaccination rates; the vertical axis (Y) is the simulated active infectious cases as a percentage of the total agents (%); the horizontal axis (X) is the day of simulation.

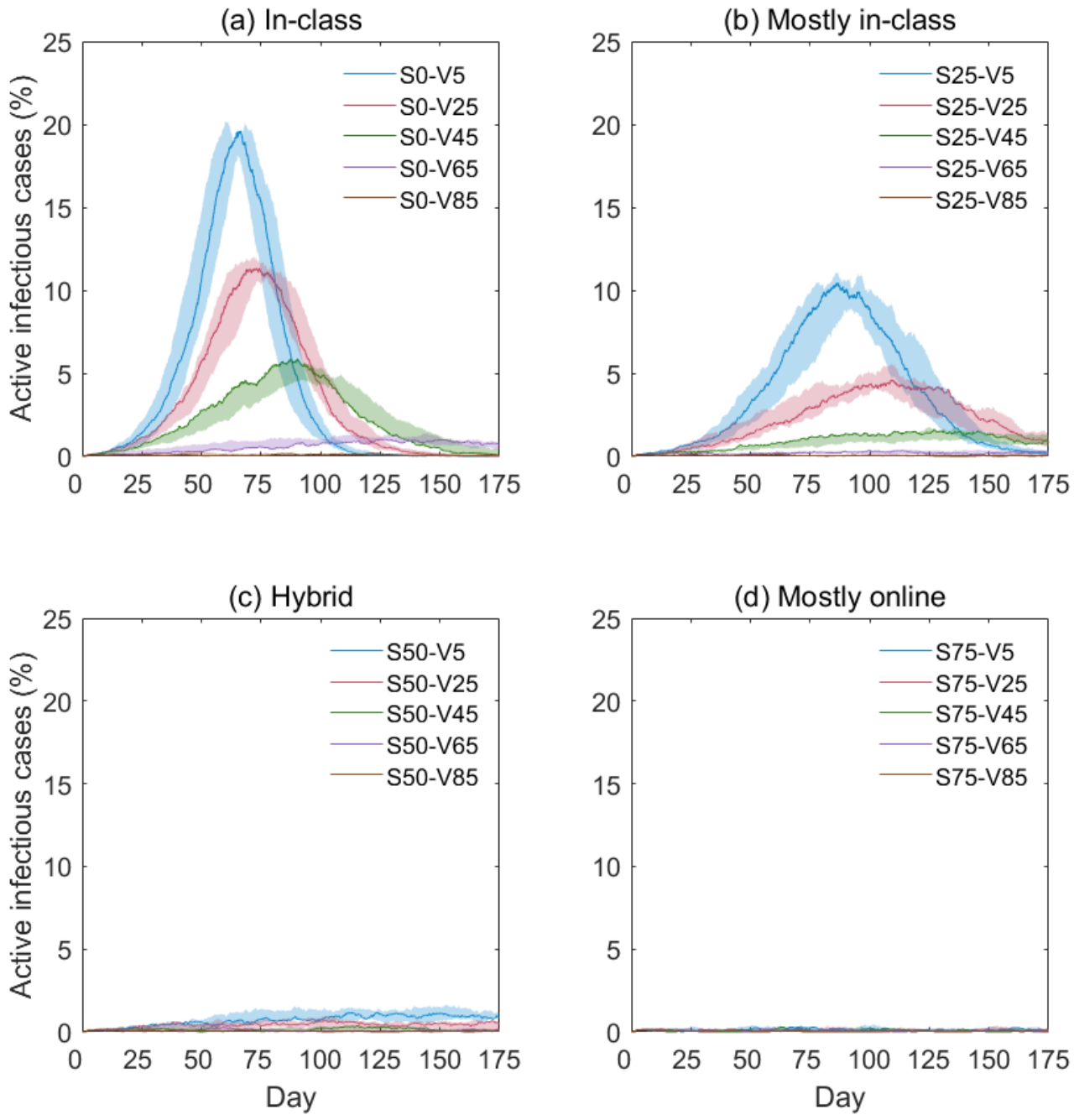

Figure 8

Simulation results under different school reopening scenarios with different teaching modalities: (a) in-class, (b) mostly in-class, (c) hybrid, and (d) mostly online. Curves in different colors represent different vaccination rates; the vertical axis (Y) is the simulated active infectious cases as a percentage of the total agents (%); the horizontal axis (X) is the day of simulation.

Supplementary Files

This is a list of supplementary files associated with this preprint. Click to download.

- SupplementaryMaterialv2.docx